C2012-0001559

NACE INTERNATIONAL CORROSION 2012 CONFERENCE & EXPO

Aspects of Localized Corrosion in an H_2S / CO_2 Environment

Bruce Brown, Srdjan Nešić
Institute for Corrosion and Multiphase Technology
Department of Chemical and Biomolecular Engineering
Ohio University
342 W. State St.
Athens, OH 45701

ABSTRACT

A 2000-liter, large scale flow loop with 10 cm I.D. pipeline and three different test sections has been used over several years with the goal of understanding the mechanisms involved in H_2S/CO_2 corrosion environments. Mild steel from an API 5L X65 pipeline was used for the flush-mounted weight loss samples in the flow loop, each was exposed to consistent test conditions for up to 3 weeks at a time. The corrosion product morphology and resulting uniform or localized corrosion are here reviewed from experiments conducted at 60°C, with partial pressures of CO_2 up to 8 bar, partial pressure of H_2S up to 10 mbar and NaCl concentrations up to 10 wt.%; tests were conducted at pH 4, 5 and 6.

Key words: hydrogen sulfide, iron sulfide, carbon dioxide, iron carbonate, localized corrosion, corrosion products.

INTRODUCTION

The ability to predict corrosion relies upon using data from the laboratory and from the field in order to develop models of the type of corrosion observed. Empirical models provide a solid starting point for capturing the effect of major parameters (pCO_2, pH_2S, acetic acid, chlorides, temperature, flow, etc.) and indicate how each of those can affect the uniform corrosion rate in upstream oil and gas pipelines. However, it is more important to be able to predict the likelihood and magnitude of localized corrosion in H_2S and CO_2/H_2S environments, which is often related to the nature or breakdown of a protective corrosion product layer and therefore it's role in development of localized attack needs to be elucidated. As more knowledge emerges and fills in gaps in a theoretical framework, development of a mechanistic model becomes possible and is the best way to describe the effect of multiple parameters involved.

The mechanistic uniform H_2S and H_2S/CO_2 corrosion prediction model used currently in MULTICORP* is based on fundamental theories and experimental results[1] aimed at describing specific mechanisms of corrosion. Built in hypotheses, which have been publicly documented,[2] are based on the current understanding of uniform H_2S and H_2S/CO_2 corrosion, such as:

1. The corrosion rate of mild steel in H_2S and CO_2/H_2S environments is affected by H_2S concentration, CO_2 partial pressure, pH, system temperature, flow velocity, and most of all by the formation/protectiveness of the iron sulfide layer.
2. When H_2S and steel are in an aqueous system, iron sulfide (mackinawite) formation rapidly occurs via a heterogeneous chemical redox reaction of H_2S with iron on the steel surface.
3. Iron sulfide (mackinawite) forms a very thin dense film at the steel surface which acts as a diffusion barrier for all species involved in the corrosion reaction. This film undergoes a cyclic process of growth, cracking, and delamination to develop an iron sulfide corrosion product layer.
4. The amount of iron sulfide retained on the steel surface depends on the layer formation rate and the layer damage rate. The iron sulfide layer forms directly by corrosion and/or by precipitation mechanisms; damage to the iron sulfide layer occurs by mechanical and/or chemical means.

In order to predict localized corrosion, there must be a solid body of understanding of the mechanisms involved in the corrosion process, especially mechanisms related to the corrosion product layer when H_2S is involved.

* Trade name for sponsor-supported, mechanistic corrosion prediction software developed at ICMT.

The set of experiments presented below is related to localized H_2S corrosion and has focused on the interaction of CO_2, H_2S, water chemistry, and fluid flow on the corrosion of mild steel. Specific environmental conditions are set and observations are made of the corrosion product layer formed to determine whether it will lead to localized corrosion. However, the biggest limitation in corrosion research is often available time. Although it is understood that time can play a significant role in the development of localized corrosion, it is hypothesized that initiation of events that will lead to a localized failure can be observed over a timeframe, of weeks rather than years. To compromise with respect to time when using a large scale sour corrosion test system such as the one in the present study, an experimental test time of 3 weeks with interim observations after1 week and 2 week exposures, has been used as a fixed timeframe, which enables direct comparison of empirical results. In this timeframe, detection of any localized corrosion is deemed possible and considered probable under large scale experimental conditions.[3, 4] Expectations from this large scale research program are that it will provide information on the range of conditions in which mild steel can undergo localized H_2S corrosion, an aid understanding of the corrosion product layer's relationship to localized corrosion. The idea is to generate key information which will help understand the mechanisms involved in localized corrosion of mild steel in sour environments, and which will assist in building better and more reliable models.

EXPERIMENTAL PROCEDURE

Environmental Conditions

Large Scale Flow Loop. A large scale flow loop with 10.1 cm I.D. pipeline was used in this work to better simulate multiphase fluid flow conditions expected in oil and gas pipeline field conditions. Operational procedures have been previously reported.[6] Briefly, the "Hydrogen Sulfide (H_2S) system" is a 2000 liter flow loop with a 1500 liter tank, two Moyno* progressive cavity pumps, 3 test sections with multiple 5 cm probe insertion locations, an in situ pH measurement side stream, a port for gas sampling and a main gas mixing panel for addition of pure gases.

The two progressive cavity pumps maintain measured flow rates of liquid and gas through the closed system with separation of the gas and liquid over a diffusion plate in the tank. Liquid flow first travels through a single phase flow (SP) test section, placed over 20 pipe diameter lengths downstream of the liquid pump, then to a mixing point for the gas and liquid streams, located 10 pipe diameters downstream from the SP test section. After the mixing point, there are two multiphase flow (MP) test sections with a minimum of 60 pipe diameter lengths of straight pipeline upstream of each; this facilitates development of the multiphase slug flow regime.

* Trade Name

Environmental Conditions. Temperature, total pressure, pH, and H_2S concentration are set prior to sample insertion. All additions to the flow loop done to control or define the environmental conditions are completed before the steel to be tested is inserted. Some additions of hydrogen sulfide are necessary during the 21 day test when maintaining the low partial pressures. Dissolved iron concentration is measured whenever possible in order to complete the water chemistry profile.

Liquid flow rate:	0.5 m/s to 2.5 m/s
Gas flow rate:	2.0 m/s to 10 m/s
Temperature range:	25°C to 90°C
Pressure range:	1 bar to 70 bar

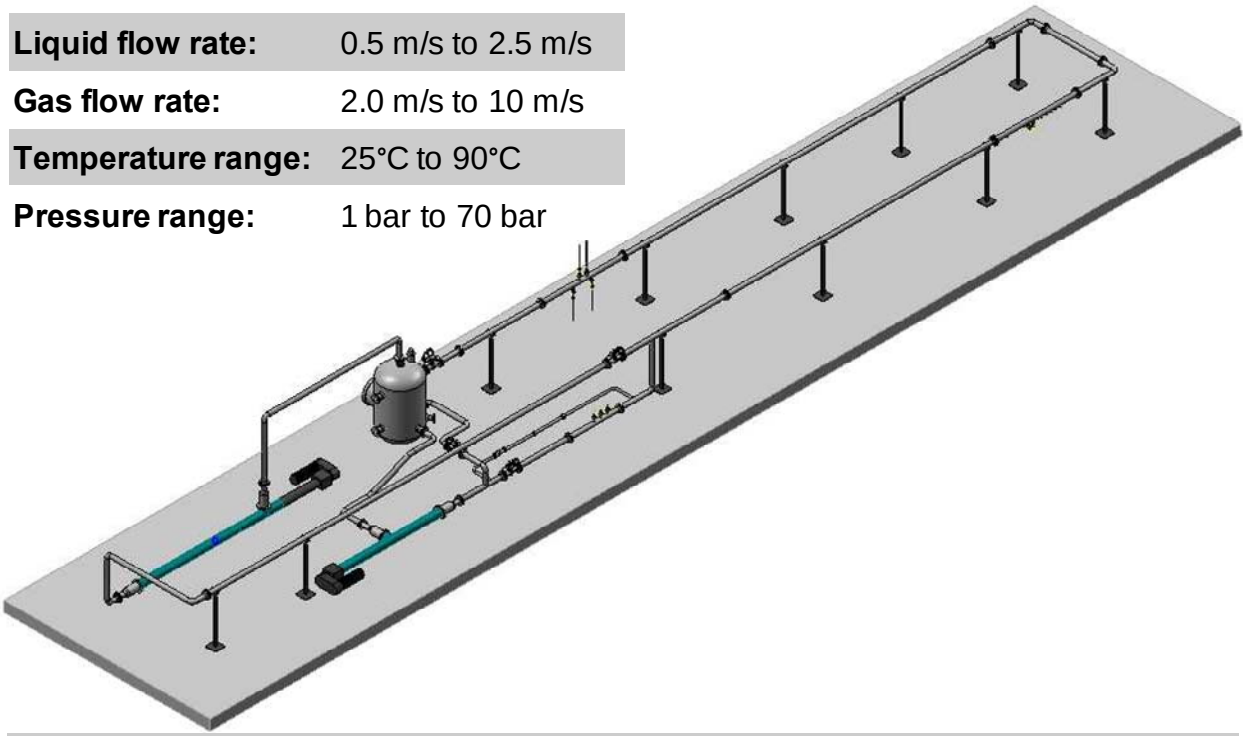

Liquid mixtures:	deionized water, salt solutions, model oil
Gas Mixtures:	N_2, CO_2, H_2S
Instrumentation:	Superficial liquid and gas velocities, flow regime determination, corrosion rate, pH, and temperature

Figure 1. H_2S Multiphase Flow Loop used in testing: 2000 liter total volume, 10.1 cm I.D. Hastelloy* line.

Multiphase Flow. For this series of tests the flow regime was set as 3 m/s superficial gas velocity (V_{sg}) and a 1 m/s superficial liquid velocity (V_{sl}) to develop slug flow with a slug frequency of approximately 1 per second. The previously referenced corrosion prediction software was also used to define conditions for the required flow regime and calculate a wall-shear stress of the slug front to be greater than 40 Pa (Figure 2). This type of flow regime was chosen to provide a consistent, repeatable, turbulent flow effect during the development of the corrosion product layer.

* Trade Name.

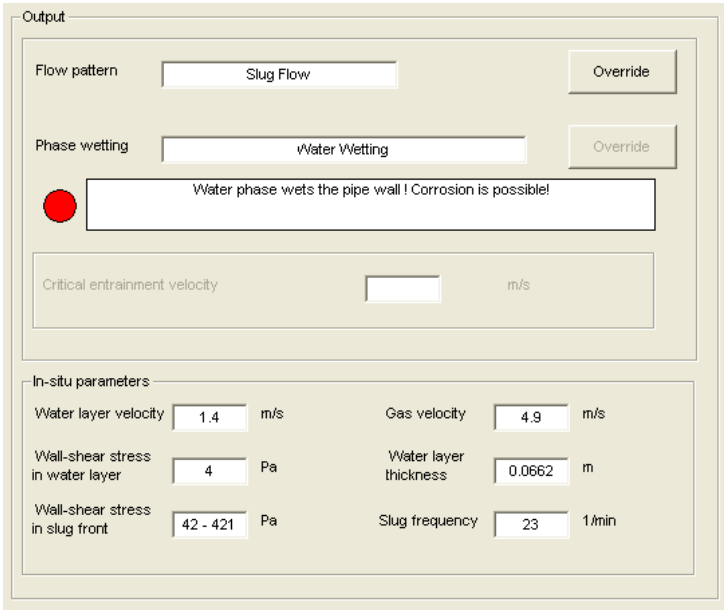

Figure 2. Output from flow prediction software for flow conditions described above.

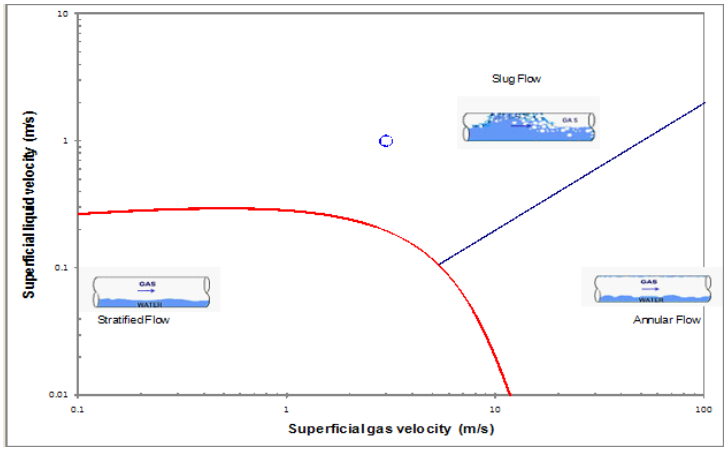

Figure 3. Flow regime map for the environment described above, showing the location of the flow conditions as an "O" in the center of the graph at V_{sl} =1 m/s and V_{sg} =3 m/s.

Corrosion Measurements

The H_2S system simultaneously holds 7 weight loss samples, 3 exposed to single phase flow (SP), and 4 in multiphase (MP) flow. The weight loss samples are made from a X-65 pipeline material (Table 1), machined into 6.35 mm (0.25 in.) thick, 31.75 mm (1.25 in.) diameter disks with a mounting hole in the middle of each. The exposed weight loss surface area is 7.4 cm^2. Each X-65 weight loss sample is subjected to the same polishing procedure, ending with a 600-grit silicon carbide paper that leaves a uniform surface for testing; polishing marks are

oriented in one direction. All samples are flush mounted to the inside wall of the 10.1 cm diameter test sections after the test conditions have been set.

Table 1. Chemical Composition of weight loss material - API 5L X65 (balance Fe).

Material Name	Al	As	B	C	Ca	Co	Cr	Cu
API 5L X65	0.032%	0.008%	0.001%	0.13%	0.002%	0.007%	0.14%	0.131%

Mn	Mo	Nb	Ni	P	Pb	S	Sb
1.16%	0.16%	0.017%	0.36%	0.009%	<0.001%	0.009%	0.009%

Si	Sn	Ta	Ti	V	Zr
0.26%	0.007%	<0.001%	<0.001%	0.047%	<0.001%

Uniform corrosion rates were determined by weight loss from the exposed surface area during sample analysis. After the samples were removed from the H_2S system and analysis of the corrosion product has been completed, the entire corrosion product layer was removed by a Clarke solution cleaning procedure method outlined in ASTM G1.[7] Weight loss for uniform corrosion rate is measured as a difference in mass before and after the experiment with no corrosion product on the samples. Pit depth was measured with an optical Alicona* Infinite Focus Microscope (IFM) after the corrosion product has been removed.

Analysis Techniques

Preparation and Procedure. Samples removed from the corrosion experiments for analysis were immediately and thoroughly rinsed with isopropyl alcohol to remove the water from the surface and limit oxidation of the corrosion product layer. All samples were then stored in a vacuum desiccator prior to the analysis process and thereafter. After drying, sample weight was recorded. The samples were first analyzed with the IFM and SEM with the film / layer intact. Samples chosen for cross-sectioning were fixed in a small container and a low viscosity epoxy was poured in to seal the corrosion product in place. Only half of each weight loss sample for cross-sectioning was fixed in epoxy, so the other half could be inspected by IFM after corrosion product layer removal.

Analysis with corrosion layer. Because of the importance of the corrosion product layer to this research, most of the effort in the analysis is spent on defining the topography and chemical make-up of this layer formed on the steel samples, in order to provide a correlation

* Trade Name.

with the corrosion process that occurred on the metal surface. The IFM was used to locate and document topographical surface features on each sample, such as surface areas with uniform coverage, a loss or gain of material, or a fault in the corrosion product. Scanning electron microscopy (SEM) with accompanying backscatter emission (BEC) and energy dispersive X-ray spectroscopy microanalysis (EDS) were used on each sample to document elemental composition and crystal morphologies.. Two cross-sections were made from each set of test samples to document the corrosion product thickness, any compositional variation and possible indications of localized corrosion.

Analysis without the layer. After analysis of the corrosion product layer was complete, samples were cleaned using the Clarke solution cleaning method[7]. The change in mass of each sample was reported as corrosion product weight. The half-sample without epoxy from cross sectioning was subjected to Clarke solution for approximately the same time as the other weight loss samples tested. The IFM was used again for documentation of topographical surface features of the metal surface without the corrosion product for each of these samples. These measurements were used to calculate localized corrosion rate (called here: penetration rate) and document the morphology of localized corrosion, if present.

Calculations

Uniform Corrosion Rate. The uniform corrosion rate was calculated by Equation (1):

$$(Uniform\_Corrosion\_Rate) = \frac{(weight\_loss)*(unit\_conversion\_factor)}{(density\_of\_iron)*(surface\_area)*(time)} \qquad (1)$$

Weight loss is measured in grams with an accuracy of ±0.0005 g. The surface area of the samples is 7.4 cm^2, the density of iron is 7.85 g/cm^3, and the time is measured in days. A unit conversion factor of 3650 produces a uniform corrosion rate value in mm/yr.

Pitting Ratio. The definition for pitting ratio used in this study is shown by Equation (2) as the ratio of the deepest localized corrosion location found by the IFM on the surface of the sample after corrosion product removal, to the uniform corrosion rate calculated by the weight loss method.

$$Pitting\_Ratio = \frac{(IFM\_Penetration\_Rate)}{(Uniform\_Corrosion\_Rate)} \qquad (2)$$

When the pitting ratio calculated by Equation (2) was greater than 5, in the present study this was considered to be localized corrosion. When values of the pitting ratio exceeded 3 this was considered as possible "initiation" of localized corrosion. However, if the so-defined localized attack covered more than 50% of the sample surface, then it was assumed that this was the initiation of severe uniform attack.

RESULTS AND DISCUSSION

Experimental Observations

The ranges of experimental conditions are listed in Table 2. Steel samples were exposed up to 21 days.

Table 2. Test matrix

Test Parameter	Test Condition
Temperature	60°C
Total Pressure	3 bar or 8 bar
Solution	1 wt% NaCl or 10 wt% NaCl
pH	4.0, 5.0, or 6.0
pH_2S	0.01 bar or 0.001 bar
pCO_2	balance

Table 3. Key environmental conditions for the samples exposed at 60°C, P_{total} = 8 bar, including pitting data (key: SP - Single Phase flow; MP - MultiPhase flow).

pH	P_{total}	pH_2S	NaCl	Flow	Exposure	Pitting Ratio	Penetration rate	Details of corrosion product layer
	bar	mbar	wt%		days		mm/y	
4	8	10	10	SP	7	3.4	36.3	Figure 4 - Figure 7
4	8	10	10	SP	21	0.30	2.6	Figure 8 - Figure 9
5	8	1	1	MP	21	0.45	3.3	Figure 10 - Figure 11
5	8	10	10	MP	22	13.6	30	Figure 12 - Figure 16
6	3	10	1	SP	21	7	2.2	Figure 17 - Figure 18
6	3	10	1	SP	21	0.8	0.2	Figure 19 - Figure 20

The examples shown below were chosen amongst a large number of samples which were generated in repeatable laboratory experiments, to document iron sulfide layer composition and morphologies which may be associated with localized corrosion. The six samples reviewed in the present paper are summarized in Table 3, which can be used as a quick reference to the key experimental conditions. It also indicates the measures related to localized corrosion (pitting) and provides pointers to a more detailed discussion of the experiments given below, which includes the surface images.

Experiment at pH 4.0 with 10 wt% NaCl

In many cases shown below, the original polishing marks made on the X-65 sample surface prior to insertion into the experimental flow system were still obvious on the upper surface of the final corrosion product layer. For a sample removed after a 7 day exposure at pH4.0, these "polish marks" can be seen in Figure 4 as multiple parallel lines across the surface. Although visually similar to the original steel surface, energy dispersive X-ray spectroscopy (EDS) suggests that the layer is likely iron sulfide, and the cracks within show that there is a significant depth to the corrosion product layer.

This type of corrosion product layer has been observed in numerous experiments and underpins the hypothesis that iron sulfide (mackinawite) formation occurs via a heterogeneous chemical redox reaction of H_2S with iron on the steel surface to form a thin film of iron sulfide. The initial film must be only microns thick in order to mimic the surface features, but must be dense enough to have the strength to maintain them as further layers form underneath.

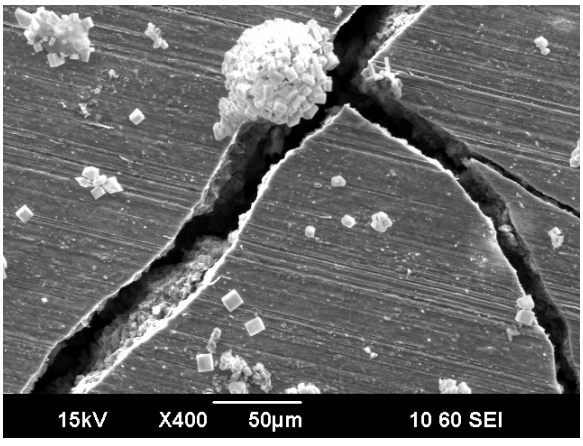

Figure 4. SEM image of polish marks visible on corrosion product layer. (60°C, pH 4.0, P_{total} = 8 bar, pH_2S = 10 mbar, 10wt% NaCl, SP, 7 days exposure)

Although the failure mechanisms of this corrosion product are not completely understood, it is known to be nonprotective with characteristics that lead to localized corrosion. Another characteristic of the corrosion product layer observed in Figure 4 is the lack of precipitates on the surface. Since the bulk conditions are undersaturated with respect to both iron sulfide and iron carbonate, any ferrous ions released in the corrosion process are expected to be locally trapped in the corrosion product layer or swept into the bulk solution.

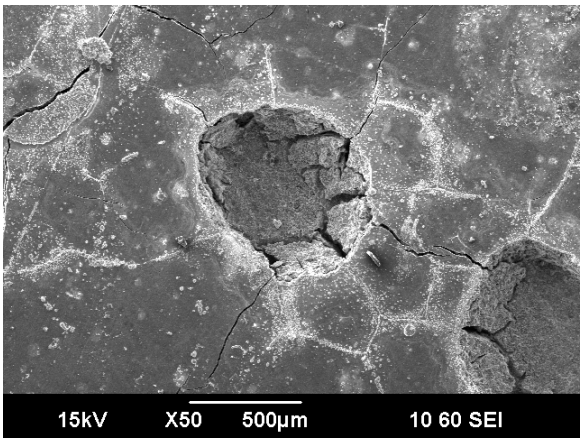

Figure 5. SEM image of failure location in corrosion product layer. (60°C, pH 4.0, P_{total} = 8 bar, pH_2S = 10 mbar, 10wt% NaCl, SP, 7 days exposure)

More breakdown of the iron sulfide corrosion product layer in bulk solutions at pH 4.0 and pH 5.0 has been observed with a typical example shown in Figure 5, as a 750 µm diameter failure in the surface layer. Further analysis with an IFM in Figure 6 quantifies the maximum depth of one of these failure locations to be 238 µm with a diameter equivalent to that shown in the SEM of Figure 5.

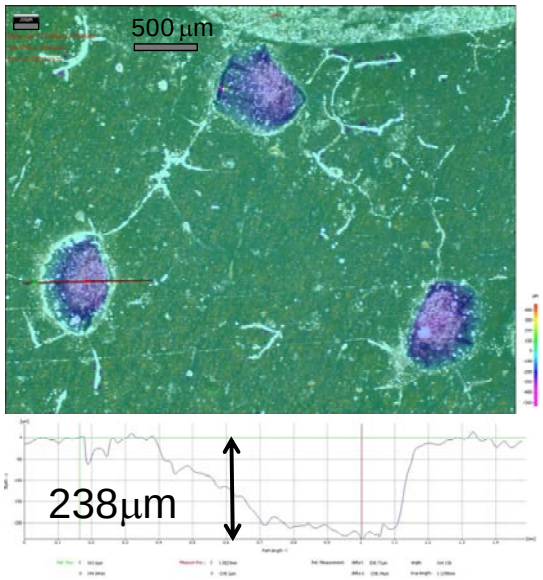

Figure 6. IFM analysis of surface features found in corrosion product layer. (60°C, pH 4.0, P_{total} = 8 bar, pH_2S = 10 mbar, 10wt% NaCl, SP, 7 days exposure)

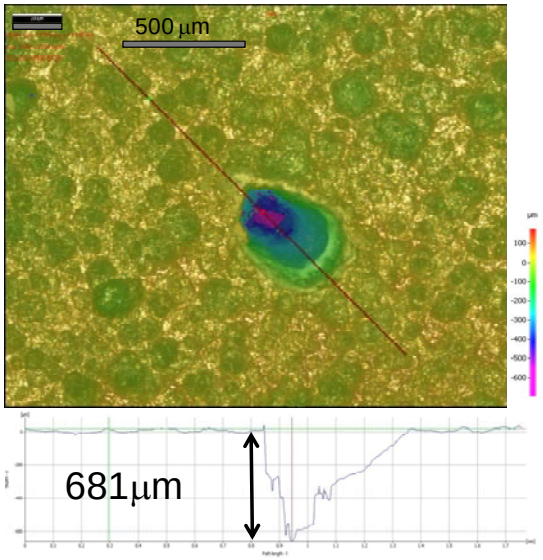

Figure 7. IFM analysis of single pit location after corrosion product layer removed. (60°C, pH 4.0, P_{total} = 8 bar, pH_2S = 10 mbar, 10wt% NaCl, SP, 7 days exposure) (pitting ratio = 3.4)

After removal of the corrosion product layer from this sample, a high uniform corrosion rate was determined to be 10.8 mm/yr by weight loss. Only one pitting location was found and was measured at 681 µm in depth (36.3 mm/yr) as shown in Figure 7, while most indications of corrosion in the substrate were consistently less than 100 µm in depth.

For a sample removed after a 21 day exposure to the same conditions at pH 4.0, "polishing marks" are still visible across the surface in Figure 8. The surface in the SEM image shows that the corrosion product layer still lacks the presence of precipitates on the surface due to undersaturated bulk conditions, although there are more sodium chloride crystals shown in this image.

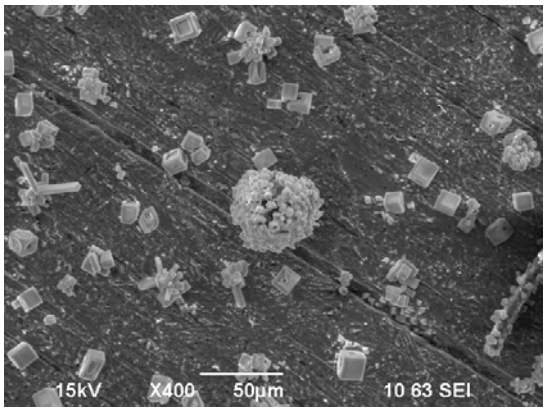

Figure 8. Polish marks visible on corrosion product layer after 21 day exposure. (60°C, pH 4.0, P_{total} = 8 bar, pH_2S = 10 mbar, 10 wt.% NaCl, MP, 21 days exposure.)

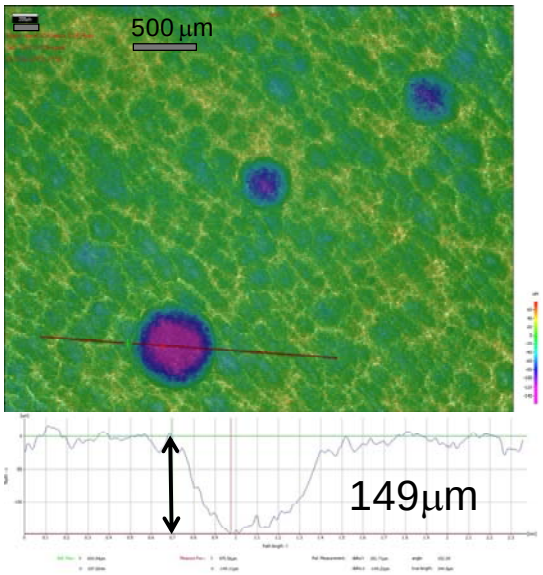

Figure 9. IFM analysis of pitting (149 μm) after corrosion product layer removed. (60°C, pH 4.0, P_{total} = 8 bar, pH_2S = 10 mbar, 10wt% NaCl, MP, 21 days exposure) (pitting ratio = 0.30)

After removal of the corrosion product layer for this sample, the uniform corrosion rate was determined to be 8.6 mm/yr by weight loss. A few pitting locations were found across the surface, similar to the 149 μm depth (2.6 mm/yr) shown in Figure 9.

In flow loop experiments at pH 4.0, each sample had visible indications of the original surface features (polishing marks) for every time exposure tested (7, 14, & 21 days). Although one sample did meet the criteria for localized corrosion in a 7 day exposure (Multiphase flow at 7 days: uniform corrosion of 10.8 mm/yr with a pit penetration rate of 36.3 mm/yr), it is hypothesized that initiation of localized corrosion that may have occurred during the short time exposure was overcome by the high uniform corrosion rates (true for 6 of the 7 weight loss samples).

Experiments at pH 5.0 with 1 wt% and 10 wt% NaCl

Experiments at pH 5.0 have shown similar corrosion product layer failure mechanisms to those found in the experiment at pH 4.0, in a 1 wt% NaCl solution at either 1 mbar or 10 mbar pH_2S, but the corrosion product surfaces do not show the characteristics of the original steel polishing marks. Figure 10 shows two different locations on the sample where the corrosion product failed. In Figure 10(a), the upper layer of corrosion product failed and presumably allowed active dissolution and corrosion of the underlying corrosion product and steel substrate, respectively. The image in Figure 10(b) shows a “dome-like” raised corrosion product layer with a “pie-shaped” missing piece. IFM analysis can only reproduce visual

images related to perpendicular measurements, so any sideways openings in a pit or a dome (*i.e.*, a cavity-like loss of material) is missed and is represented by a line. The IFM photos of these failure locations also show the visual difference between the top layer and the underlying layer of corrosion product.

After the corrosion product was removed from the sample, indications of corrosion were seen on the metal surface. Measurements with the IFM (Figure 11) of material loss up to 188 μm in depth after 21 days show this corrosion to be the initiation of uniform corrosion, since the uniform corrosion rate by weight loss (7.3 mm/yr) is more than twice the measured IFM values (3.3 mm/yr).

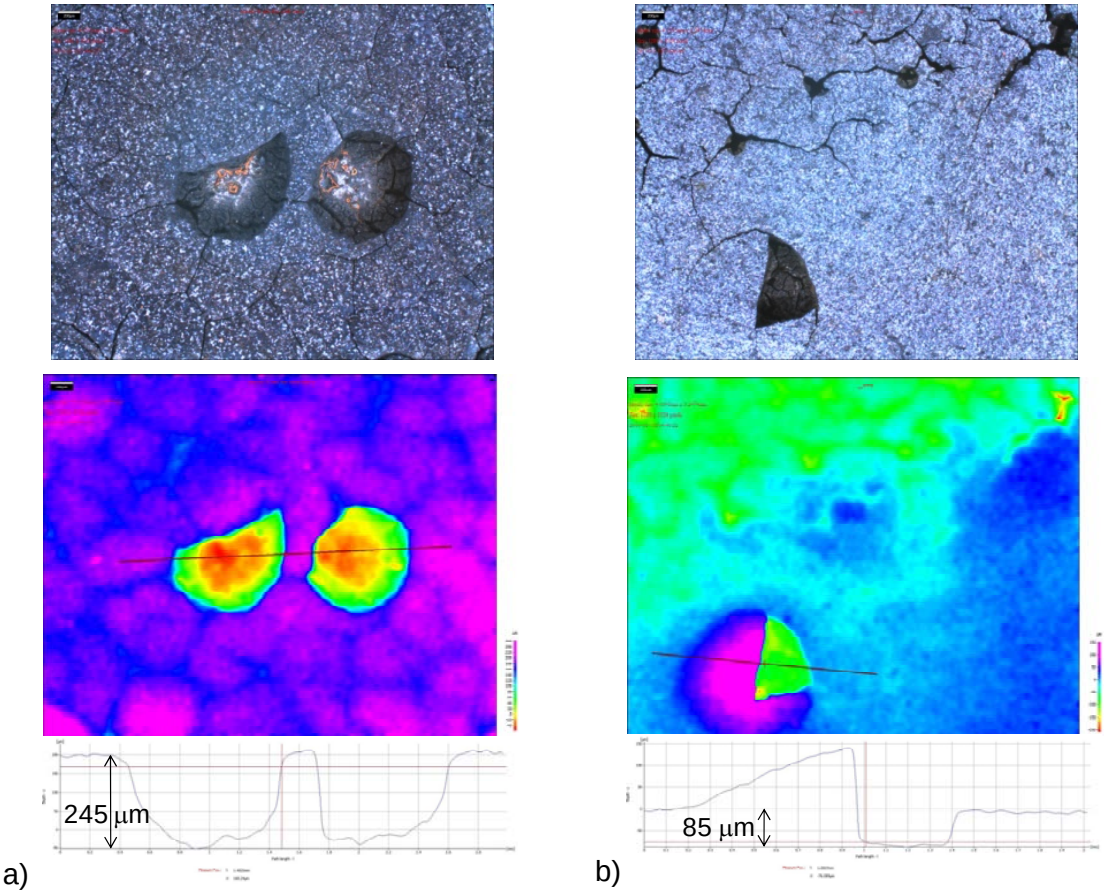

Figure 10. IFM images and analysis of the corrosion product layer showing (a) open pit failures up to 245 μm in depth [1.2 & 1.0 mm diameter, L to R] and (b) a partial layer failure with a raised corrosion product layer [1.3 mm diameter]. (60°C, pH 5.0, P_{total} = 8 bar, pH_2S = 1 mbar (100 ppm H_2S), 1wt% NaCl, MP, 21 days exposure)

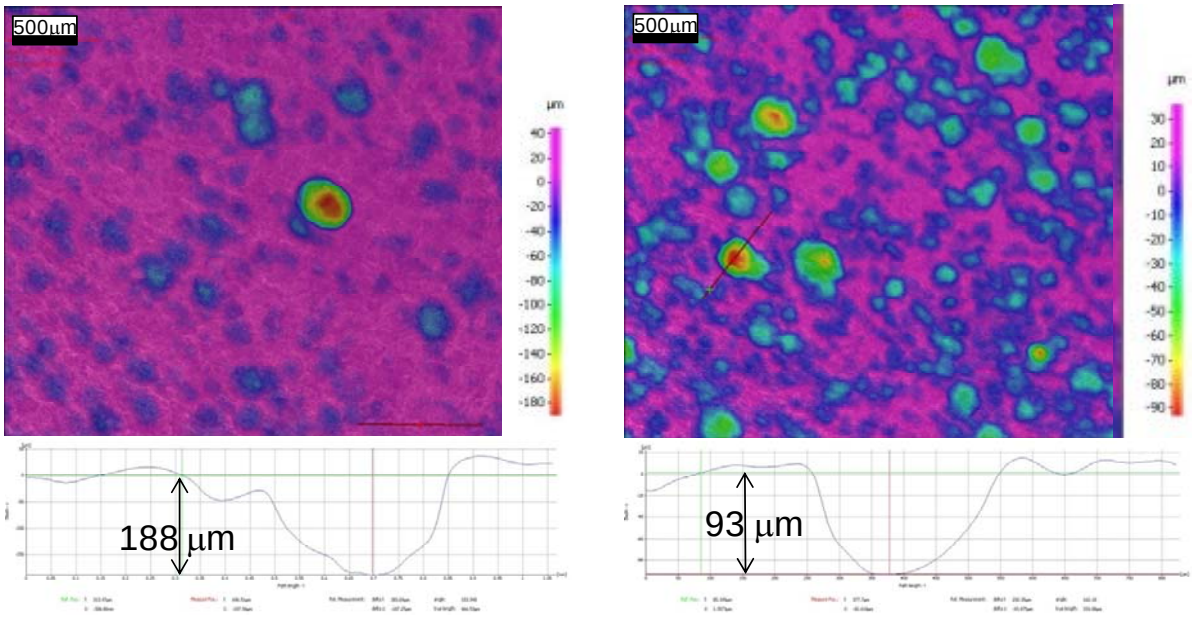

Figure 11. IFM analysis of sample surface after corrosion product layer was removed. (pH 5.0, 60°C, P_{total} = 8 bar, pH_2S = 1 mbar, 1wt% NaCl, MP, 21 days.) (pitting ratio = 0.45)

Two WL samples that were exposed to the same conditions for the entire 22 day test were both analyzed in cross section and show very high corrosion rates as well, but have remarkably different features. Figure 12, Figure 13, and Figure 14 refer to the first of these two WL sample. The surface of this sample, Figure 12, still exhibits the original polish marks on the surface, yet it can be seen that corrosion product layer has a significant depth, as indicated by the broken edge of the corrosion product layer shown in the SEM image. EDS analysis confirms a high sulfur content of the layer (likely some form of iron sulfide).

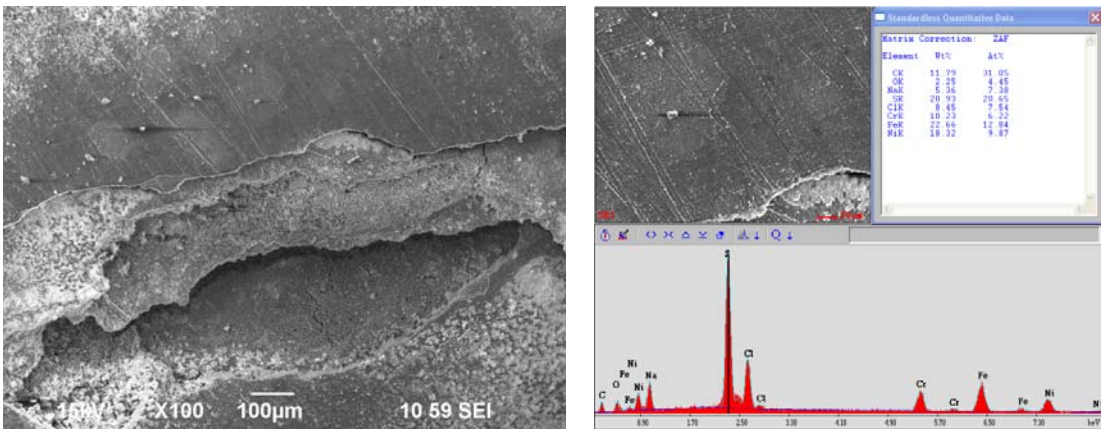

Figure 12. SEM and EDS of sample taken from multiphase flow after 22 days. Multiphase weight loss sample taken from 60°C, pH 5.0, pCO_2 = 7.7 bar, pH_2S = 10 mbar, 10 wt% NaCl (C – 11.79 wt%, O – 2.25 wt%, Na – 5.36 wt%, S – 20.93 wt%, Cl – 8.45 wt%, Cr – 10.23 wt%, Fe – 22.66 wt%, Ni – 18.32 wt%)

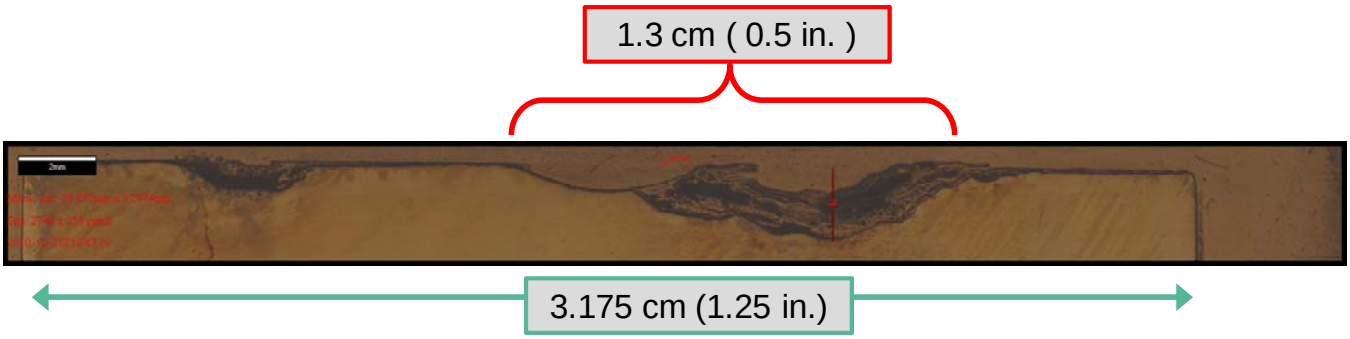

Figure 13. IFM image of the whole cross-section of the multiphase sample taken at 22 days. Multiphase weight loss sample taken from 60°C, pH 5.0, pCO_2 = 7.7 bar, pH_2S = 10 mbar, 10 wt% NaCl

This sample also has a large 1.3 cm (0.5 in.) area of localized corrosion that was too large to show in a single SEM image, so the image of the entire gold-coated cross sectional sample was captured by the IFM and shown in Figure 13. Note the three localized areas of attack on the sample surface. The one to the farthest right still contains the corrosion product layer and has a measured depth of 1.8 mm giving a 30 mm/yr penetration rate.

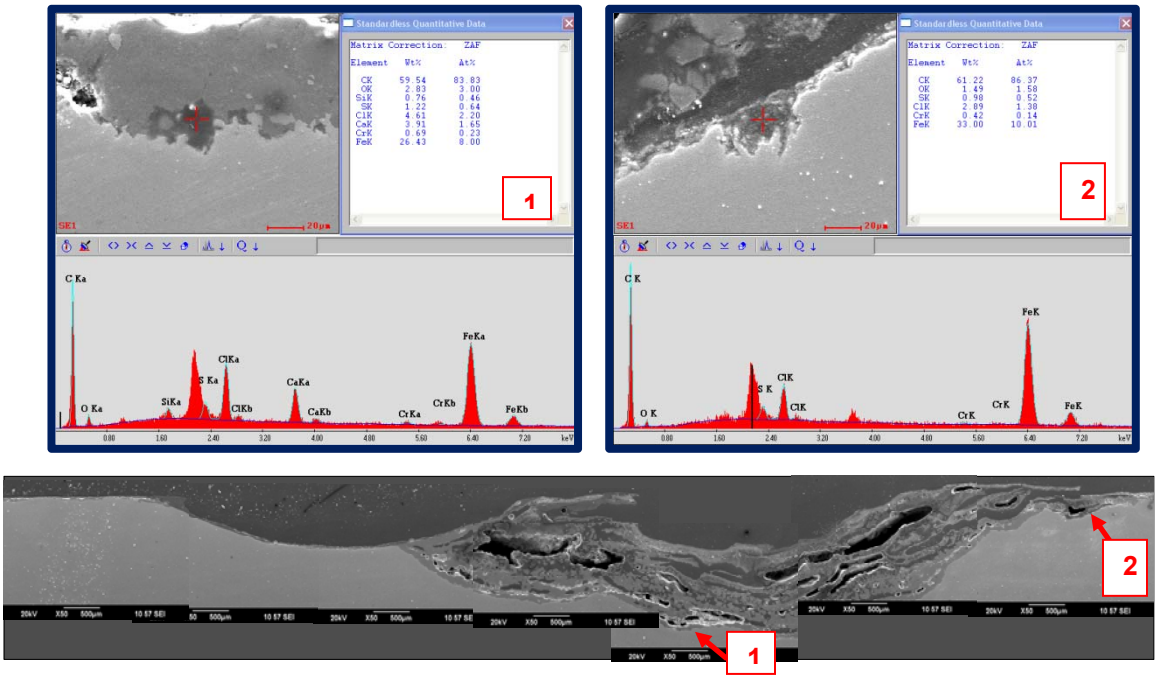

Figure 14. SEM composite image of Multiphase weight loss sample taken from 60°C, pH 5.0, pCO_2 = 7.7 bar, pH_2S = 10 mbar, 10 wt% NaCl. Arrow locations 1& 2 were analyzed by EDS. Both locations show a higher chloride content than was observed elsewhere on the same sample. [1. (C – 59.54 wt%, O – 2.83 wt%, Si – 0.76 wt%, S – 1.22 wt%, Cl – 4.61 wt%, Ca – 3.91 wt%, Cr – 0.69 wt%, Fe – 26.43 wt%)]; [2. (C – 61.22 wt%, O – 1.49 wt%, S – 0.98 wt%, Cl – 2.89 wt%, Cr – 0.42 wt%, Fe – 33.00 wt%)]

This sample had a weight loss of 0.78 grams (including the corrosion product) for a uniform corrosion rate of 2.2 mm/yr for a 13.6 pitting ratio. It can be safely assumed that the entire weight loss of this sample was related to localized corrosion.

An attempt to image the main pit by SEM is shown as a collection of SEM images and two EDS analyses in Figure 14. From these SEM images, the corrosion product in the pit shows a very porous structure with layers that do not seem to be well attached to the adjacent layer below. A lifted section of the corrosion product can be observed on the upper right of Figure 14. Another interesting feature of the corrosion product layer that can be speculated to relate to the low uniform corrosion rate of the sample is the thin layer of corrosion product (iron sulfide) covering the flat portion of the upper left of the SEM in Figure 14, thought to represent the original metal surface, and covering the 4.5 mm wide pit in the left half of the image.

The EDS spot analysis shown in Figure 14, taken at locations 1 & 2 in the overall image, shows two locations where chloride levels were measureable in the corrosion product at the metal surface. The EDS image on the right side was the first to be discovered as it is visually indicative of a location corroding more within the pit or a propagation point within the pit. The only difference in the EDS analysis at this location was the chloride peak which prompted further EDS spot checks along the bottom of the pit. Only these two locations show a peak for chlorides in the analysis. Chlorides are thought to be involved in the pit propagation process, but measured observations of this phenomenon in cross sectional analysis are usually discounted because of possible trapping that could occur during the dehydration and the cross sectional sample preparation procedure.

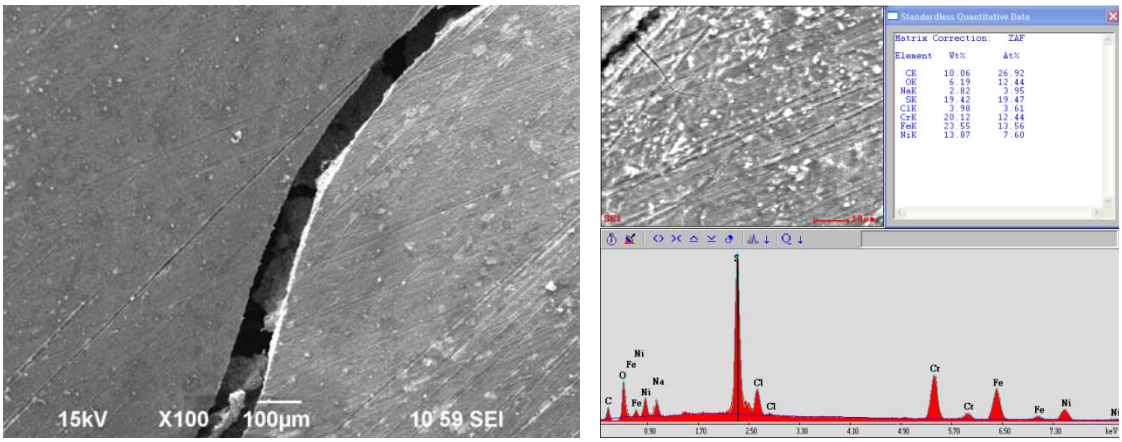

Figure 15. Sample surface after removal from H_2S system after 22 days exposure in multiphase flow. 60°C, pH 5.0, pCO_2 = 7.7 bar, pH_2S = 10 mbar, 10 wt% NaCl (C – 10.06 wt%, O – 6.19 wt%, Na – 2.82 wt%, S – 19.42 wt%, Cl – 3.98 wt%, Cr – 20.12 wt%, Fe – 23.55 wt%, Ni – 13.87 wt%)

Figure 15 and Figure 16 refer to a second WL sample taken from multiphase flow after 22 days from the same experiment. Mass loss of this sample (3.27 g, including the corrosion product

layer) equates to a 9.4 mm/yr uniform corrosion rate. Even with this amount of mass loss, the corrosion product layer shows the polish marks of the original surface (Figure 15).

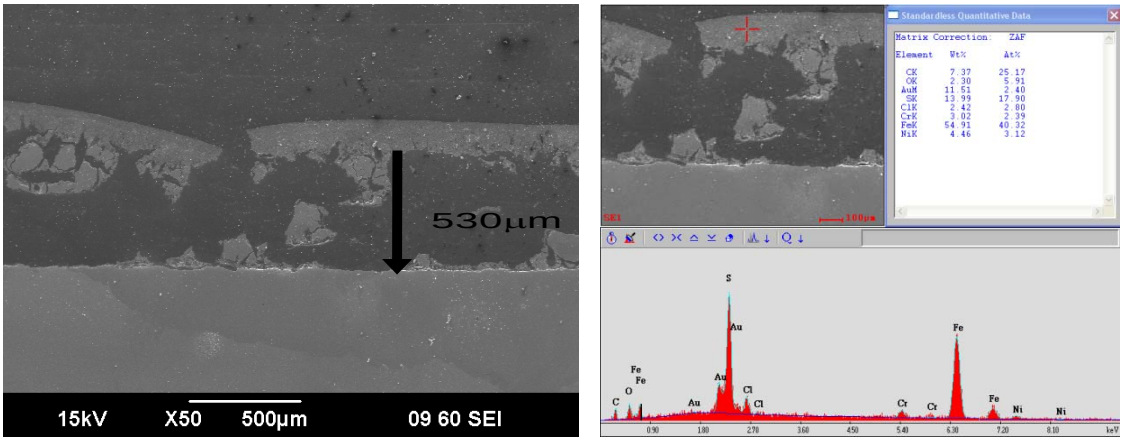

Figure 16. Cross section of multiphase sample taken after 22 days exposure. 60°C, pH 5.0, pCO_2 = 7.7 bar, pH_2S = 10 mbar, 10 wt% NaCl. (Sample mass loss = 3.27g, Corrosion rate calculation = 9.4 mm/yr. Uniform corrosion loss of substrate would be 530µm.) (C – 7.37 wt%, Au – 11.51 wt%, S – 13.99 wt%, Cl – 2.42 wt%, Cr – 3.02 wt%, Fe – 54.91 wt%, Ni – 4.46 wt%)

EDS analysis of this sample found a high sulfur peak, suggesting presence of sulfide as expected. Figure 16 shows the cross-sectional analysis image from the SEM. Note the open area between the corrosion product layer and the substrate (filled with epoxy). A detached layer was continuous across the full cross section of this sample, so, assuming uniform loss of material, the depth of uniform corrosion would be 530 µm which is visually shown as being the same as the undermined material loss in Figure 16. Observations of original surface features (with polishing marks) in micron thick corrosion product layers indicate that a thin corrosion product film formed first, but allowed corrosion to continue underneath. This was documented as well for samples with ~10 mm/yr uniform corrosion. The increased corrosion rate presumably occurred during the last 15 days of the test. The only sample meeting the criteria for localized corrosion was in multiphase flow at 7 days (0.3 mm/yr uniform corrosion and a 2.0 mm/yr penetration rate).

Experiment at pH 6.0 with 1wt% NaCl

When the system is set at pH 6.0, the surface features of each weight loss sample are affected by iron sulfide precipitation. Under these experimental conditions, iron sulfide is highly saturated in solution with just a small amount of ferrous ions (< 1ppm). Any ferrous ions that diffuse away from the metal surface react with the sulfide species in solution to form an iron sulfide precipitate. By comparison to previously reviewed surface features, weight loss samples from experiments at pH 6.0 show an increased growth of iron sulfide above the

original thin film so that none of the original surface features (i.e., “polishing marks”) can be found.

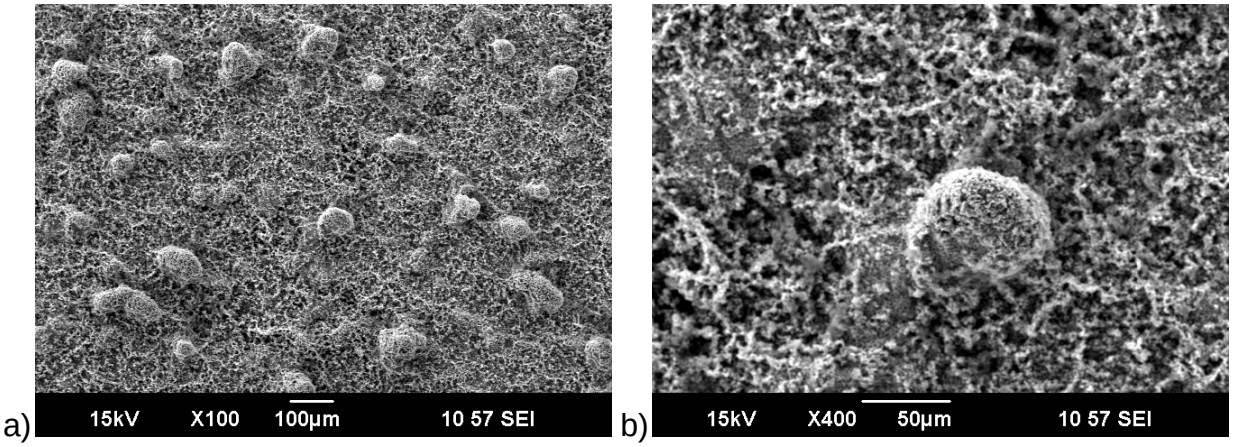

Figure 17. SEM of iron sulfide growth, Single phase flow, 21 days, 60°C, pH 6.0, pCO_2 = 2.8 bar, pH_2S = 10 mbar, 1 wt% NaCl [(a) 100x magnification, (b) 400x magnification]

WL samples exposed for 21 days experiment time did not show excessive uniform corrosion, but were still confirmed as having excess corrosion product where the localized corrosion initiation occurred. An interesting effect of preciptation was observed from the single phase test where small ‘nodes’ of iron sulfide about 50 to 100 µm in diameter grew randomly across the surface (Figure 17a). Closer visual analysis of these ‘nodes’ (Figure 17b) show small crystalline structures similar to the rest of the iron sulfide layer.

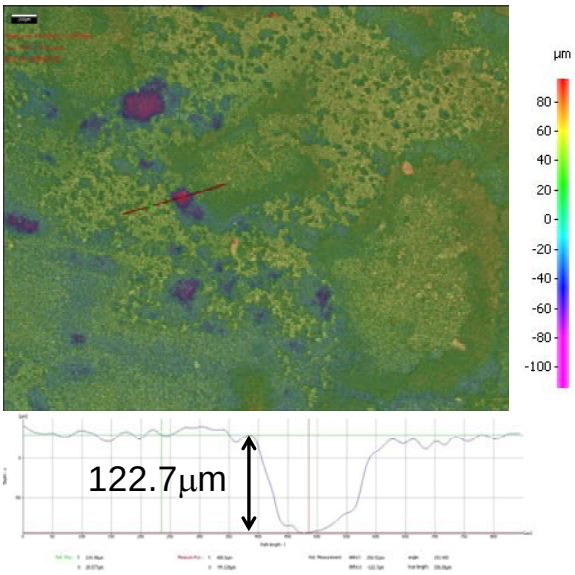

Figure 18. IFM analysis of sample WITHOUT corrosion product layer. Single phase flow, 21 days, 60°C, pH 6.0, pCO_2 = 2.8 bar, pH_2S = 10 mbar, 1 wt% NaCl (pit penetration rate = 2.2 mm/yr; uniform corrosion rate = 0.3 mm/yr; pitting ratio = 7).

After removal of the corrosion product by Clarke solution (Figure 18), localized areas of corrosion were observed in relative proportion to the nodes that were on the corrosion layer surface. With a uniform corrosion rate of 0.3 mm/yr, the pit depth measurement of 122.7 μm is equivalent to a 2.2 mm/yr pit penetration rate for a pitting ratio of 7.

a) 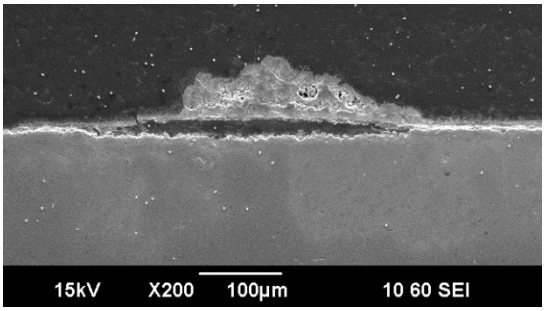

b) 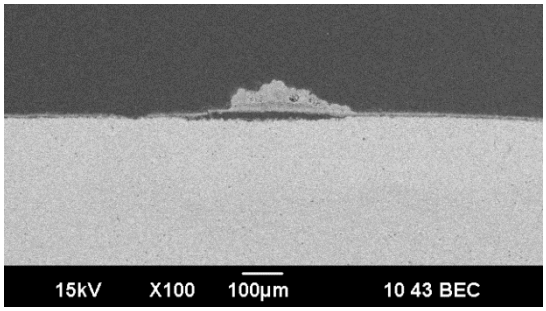

Figure 19. SEM (a) and Backscatter (b) images in cross-section analysis of localized corrosion. SP, 21 days, 60°C, pH 6.0, pCO_2 = 2.8 bar, pH_2S = 10 mbar, 1 wt% NaCl.

Another interesting feature of the corrosion product layer was observed in the cross section of a second WL sample taken from the single phase flow test section after 21 days. Most of the surface in the cross section is covered with a thin film of approximately 5 to 10 μm which is thought to limit the uniform corrosion rate by limiting mass transfer of species in both directions. This thin film can be observed in the SEM image, Figure 19a, on the extreme right and left of the image and is confirmed to be uniform over a larger area in the backscatter image, Figure 19b.

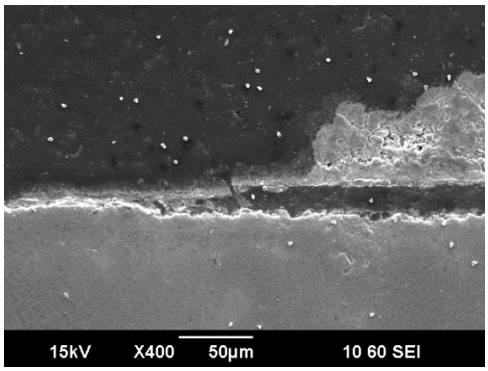

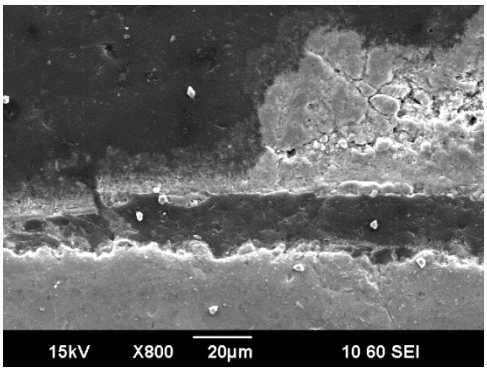

Figure 20. Close up view of SEM cross-section analysis view of localized corrosion showing continued growth of iron sulfide precipitation layer. (SP, 21 days, 60°C, pH 6.0, pCO_2 = 2.8 bar, pH_2S = 10 mbar, 1 wt% NaCl)

The localized corrosion location shows the growth of corrosion product layer and upon closer examination in Figure 20, the continued growth of iron sulfide is observed as a very light color change in the epoxy above the corrosion product.

What was not observed in any of the corrosion product analysis for these test conditions was the presence of the original polishing marks on the top surface. This is of interest because the changes in bulk chemistry parameters of this experiment have caused a change in the layer growth mechanisms. It is also noted that localized corrosion was observed where the corrosion product growth had exceeded that of the surrounding area.

CONCLUSIONS

From experiments conducted over a wide range of experimental parameters in a large scale multiphase flow system, observations were made related to failure of iron sulfide corrosion product layers and the associated localized corrosion attack:

1. Observation and analysis confirm the hypothesis that H_2S will react rapidly with a mild steel surface in aqueous solutions to form an iron sulfide layer which presents a diffusion barrier for all species involved in the corrosion process.
2. New corrosion product layers continuously form underneath the previously formed layer as corrosion proceeds. When the supersaturation of the bulk solution is exceeded, precipitation of iron sulfide from the solution side of the corrosion product layer is also seen.
3. Incidence of corrosion product layer failure coincides with localized corrosion observations, however a cause for this behavior is still not fully understood.

ACKNOWLEDGEMENTS

The author would like to thank the following companies for their financial support: BG Group, BP, Champion Technologies, Chevron, Clariant Oil Services, ConocoPhillips, Encana, ENI S.p.A., ExxonMobil, WGIM, NALCO Energy Services, Occidental Petroleum Co., Petrobras, PETRONAS, PTT, Saudi Aramco, INPEX Corporation, Total and TransCanada.

REFERENCES

1. Sun, W., "Kinetics of Iron Carbonate and Iron Sulfide Scale Formation in CO_2/H_2S Corrosion," PhD Dissertation, Russ College of Engineering and Technology of Ohio University, Nov. 2006

2. Sun, W., and Nesic, S., "A Mechanistic Model of Uniform Hydrogen Sulfide/Carbon Dioxide Corrosion of Mild Steel," Corrosion, 65 (2009), 291-307.

3. Brown, B., "H_2S/CO_2 Corrosion in Multiphase Flow," Institute for Corrosion and Multiphase Technology Board Meeting, confidential reports, March 2006 & October 2006.

4. Brown, B., "H_2S/CO_2 Corrosion at High Salt Concentration," Institute for Corrosion and Multiphase Technology Board Meeting, confidential report, October 2007.

5. Brown, B., Young, D., Nesic, S., "Localized Corrosion in an H2S / CO2 Environment," Paper No. 2704, ICC 2008, Las Vegas, NV.

6. Brown, B., Schubert, A., "The Design and Development of a Large-Scale Multiphase Flow Loop for the Study of Corrosion in Sour Gas Environments," NACE Corrosion 2002, paper no. 02502.

7. ASTM Standard G1, 2003, "Standard Practice for Preparing, Cleaning, and Evaluating Corrosion Test Specimens," ASTM International, West Conshohocken, PA, 2003, DOI: 10.1520/G0001-03, www.astm.org.

8. Benning, L.G., Wilkin, R.T., Barnes, H.L., "Reaction pathways in the Fe-S system below 100ºC," Chemical Geology, v. 167, 2000, pp25-51

9. Shoesmith, D. W., Taylor, P., Bailey, M.G., and Owen, D.G., "The formation of ferrous monosulfide polymorphs during the corrosion of iron by aqueous hydrogen sulfide at 21°C," Journal of Electrochemical Society, 125 (1980) 1007-1015.

10. Brown, B., Nesic, S., and Parakala, S.R., "CO_2 corrosion in the presence of trace amounts of H_2S," paper no. 04736, NACE International, Houston, Texas, 2004.

11. Smith, S., Brown, B., Sun, W., "Corrosion at Higher H_2S Concentrations and Moderate Temperatures," NACE Corrosion 2011, paper no. 11081,